A Study of the Electronic Spin-State Crossover in $\{Fe[HC(3,4,5\text{-}Me_3pz)_3]_2\}(BF_4)_2$

Daniel L. Reger,*[a] J. Derek Elgin,[a] Mark D. Smith,[a] Fernande Grandjean,[b] Leila Rebbouh,[b] and Gary J. Long*[c]

Keywords: Iron / N ligands / Spin crossover / Magnetic properties / Mössbauer spectroscopy

The synthesis, structural, magnetic, and Mössbauer spectroscopic properties of $\{Fe[HC(3,4,5\text{-}Me_3pz)_3]_2\}(BF_4)_2$ are reported. The single-crystal X-ray structure results indicate that at 150 K $\{Fe[HC(3,4,5\text{-}Me_3pz)_3]_2\}(BF_4)_2$ has a structure which is very similar to that observed at 220 K for the trigonally distorted octahedral, high-spin $\{Fe[HC(3,5\text{-}Me_2pz)_3]_2\}(BF_4)_2$ complex. Both the magnetic and Mössbauer spectroscopic results indicate that $\{Fe[HC(3,4,5\text{-}Me_3pz)_3]_2\}(BF_4)_2$ is high spin between 160 and 296 K. Upon cooling, $\{Fe[HC(3,4,5\text{-}Me_3pz)_3]_2\}(BF_4)_2$ exhibits a complete electronic spin-state crossover from the high-spin to the low-spin state at approximately 110 K and remains completely low spin down to 4.2 K; upon subsequent warming from 4.2 K, the transition from the low-spin to the high-spin state occurs at 148 to 150 K. $\{Fe[HC(3,4,5\text{-}Me_3pz)_3]_2\}(BF_4)_2$ exhibits a rather large thermal hysteresis of 38 K in its spin-state crossover. Thus, $\{Fe[HC(3,4,5\text{-}Me_3pz)_3]_2\}(BF_4)_2$ behaves differently from both $\{Fe[HC(3,5\text{-}Me_2pz)_3]_2\}(BF_4)_2$, which is known to show a unique spin-state crossover of one-half of its iron(II) ions associated with a phase transition, and $Fe[HB(3,4,5\text{-}Me_3pz)_3]_2$, which is known to remain high-spin even upon cooling to 1.7 K.

Introduction

The various unsubstituted and methyl-substituted tris(pyrazolyl)borate anionic ligands[1] have become very important in coordination chemistry and are known to sometimes provide a crystal-field potential that leads to a spin-state crossover in nominally octahedral high-spin iron(II) complexes.[2−4] This crossover, which involves a change from the paramagnetic $^5T_{2g}$ high-spin state to the diamagnetic $^1A_{1g}$ low-spin state, can be induced by cooling, by optical excitation, or by the application of pressure.[5−9]

The ubiquity of the tris(pyrazolyl)borate ligands in yielding a variety of electronic spin-state behaviors in iron(II) complexes led us to undertake an extensive investigation of the iron(II) complexes formed with the related unsubstituted and methyl-substituted tris(pyrazolyl)methane neutral ligands.[10−17] This work showed different behaviors for $\{Fe[HC(3,5\text{-}Me_2pz)_3]_2\}(BF_4)_2$ and $\{Fe[HC(3,5\text{-}Me_2pz)_3]_2\}I_2$: the first complex exhibits[10−13] a unique structural phase transition upon cooling, a phase transition that induces a spin-state crossover to the low-spin state of only one-half of the initially identical high-spin iron(II) ions; in contrast, the second complex exhibits[14−15] the more usual complete spin-state crossover upon cooling and at high-pressure. Interestingly, the low-spin complex, $\{Fe[HC(pz)_3]_2\}(BF_4)_2$, undergoes a gradual spin-state transition[11] to the high-spin state upon heating above 295 K, a transition which is very similar to that observed[7] in the analogous borate complex, $Fe[HB(pz)_3]_2$.

We have undertaken an investigation of $\{Fe[HC(3,4,5\text{-}Me_3pz)_3]_2\}(BF_4)_2$ (**1**) for two reasons: because $Fe[HB(3,4,5\text{-}Me_3pz)_3]_2$ is known[7] to remain high-spin even upon cooling to 1.7 K and to show a spin-state crossover to the low-spin state at high pressure,[7] and because $\{Fe[HC(3,5\text{-}Me_2pz)_3]_2\}(BF_4)_2$ has a unique spin-state crossover behavior. Herein we report the synthesis, the single-crystal X-ray structure and magnetic analysis, and Mössbauer spectroscopic studies of this new complex, a complex that does show a complete spin-state crossover from the high-spin to the low-spin state upon cooling.

Results and Discussion

Synthesis

The reaction of $Fe(BF_4)_2\cdot 6H_2O$ and two equivalents of $HC(3,4,5\text{-}Me_3pz)_3$ prepared according to a modified literature procedure[18] in tetrahydrofuran leads to the formation of $\{Fe[HC(3,4,5\text{-}Me_3pz)_3]_2\}(BF_4)_2$ (**1**), see Scheme 1.

[a] Department of Chemistry and Biochemistry, University of South Carolina, Columbia, SC 29208, USA
[b] Institute of Physics, B5, University of Liège, 4000 Sart-Tilman, Belgium
[c] Department of Chemistry, University of Missouri-Rolla, Rolla, MO 65409-0010, USA

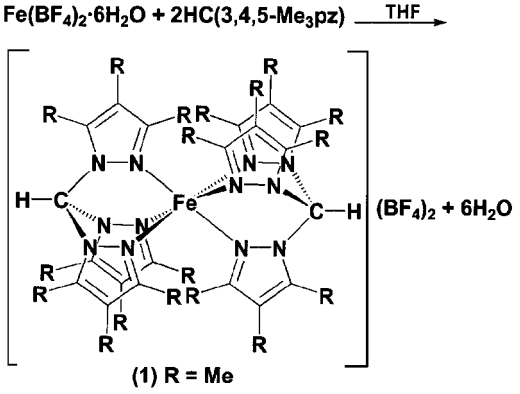

Scheme 1

$\{Fe[HC(3,4,5\text{-}Me_3pz)_3]_2\}(BF_4)_2$ in powder form is white, and its single crystals are colorless indicating that the iron(II) is high-spin at room temperature.[8,11] The solution phase ^1H NMR spectrum is broad with chemical shifts ranging from 41 to −43 ppm, a range that is indicative of a paramagnetic high-spin iron(II) complex.

X-ray Structure

The single-crystal X-ray structure of the iron(II) cation in **1** is shown in Figure 1 and a view down the H−C−Fe−C−H pseudo-threefold axis of the cation is shown in Figure 2. Crystallographic information and selected bond lengths and angles are given in Table 1 and Table 2. The structure of the N_6 coordination environment is that of a distorted octahedron in which the largest structural deviation results from the restrictions imposed by the chelate rings; the intraligand N−Fe−N angles average 84.1°. The average Fe−N bond length is 2.162 Å, a value that is clearly indicative of a high-spin iron(II) complex. In contrast, an average Fe−N bond length of about 1.97 Å is typical of a low-spin iron(II) complex with an N_6 coordination environment.[3] The structure of the cation in **1** is very similar to that in $\{Fe[HC(3,5\text{-}Me_2pz)_3]_2\}(BF_4)_2$. In this complex the average Fe−N bond length is 2.17 Å and the chelate rings restrict the intraligand N−Fe−N angles to an average of 84.3°.[11]

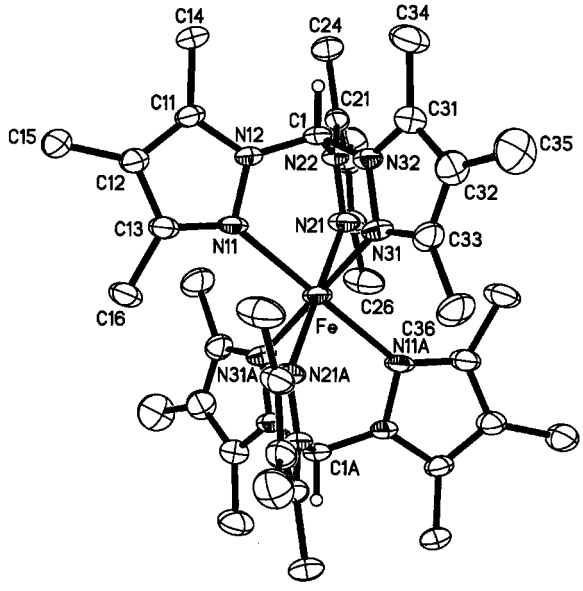

Figure 1. The structure of the cation in $\{Fe[HC(3,4,5\text{-}Me_3pz)_3]_2\}(BF_4)_2$ (**1**) with atom numbering

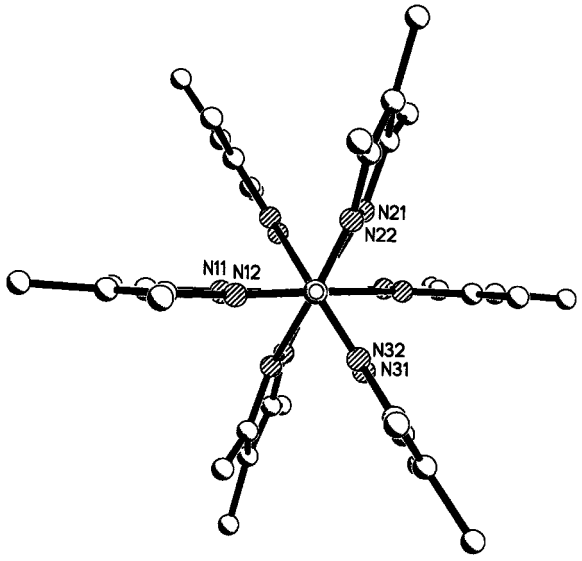

Figure 2. A view down the H−C−Fe−C−H pseudo-threefold axis of the cation in $\{Fe[HC(3,4,5\text{-}Me_3pz)_3]_2\}(BF_4)_2$ (**1**)

Table 1. Crystallographic data for $\{Fe[HC(3,4,5\text{-}Me_3pz)_3]_2\}(BF_4)_2$ (**1**)

Formula	$C_{38}H_{56.7}B_2F_8FeN_{12}O_{0.35}$
Molecular mass (g mol^{-1})	916.72
Space group	$P-1$
Crystal system	triclinic
a (Å)	10.5451(5)
b (Å)	10.8148(6)
c (Å)	11.0021(6)
α (deg)	83.4960(10)
β (deg)	88.5220(10)
γ (deg)	63.4790(10)
V (Å^3)	1115.02(10)
Z	1
Crystal color, habit	colorless, block
$D_{calcd.}$ (g cm^{-3})	1.364
Temperature (K)	150(1)
Diffractometer	Bruker SMART APEX CCD
Radiation	Mo-K_α (λ = 0.71073 Å)
$R(F)$ (%)[a]	4.75
$R(wF^2)$ (%)[a]	12.17

[a] Quantity minimized: $R(F) = \Sigma[F_o - F_c]/\Sigma[F_o]$; $R(wF2) = \Sigma[w(F_o^2 - F_c^2)^2]/\Sigma[(wF_o^2)]^{1/2}$.

One interesting difference between the two structures involves the "tilting" of the pyrazolyl rings away from an ideal C_{3v} arrangement. In the absence of tilting the FeN(n1)−N(n2)−C(n1) torsion angles (where n denotes the ring number) would be 180° and the iron(II) ion would reside in the planes defined by the pyrazolyl rings. In general, this torsion angle decreases as the size of the metal ion in-

Table 2. Selected bond lengths and angles in {Fe[HC(3,4,5-Me$_3$pz)$_3$]$_2$}(BF$_4$)$_2$ (**1**)

Bond lengths (Å)	
Fe−N(31)	2.150(2)
Fe−N(21)	2.159(2)
Fe−N(11)	2.1784(19)
C1−N(32)	1.436(3)
C1−N(12)	1.439(3)
C1−N(22)	1.445(3)
Bond angles (°)	
N(31)−Fe−N(21)	83.25(8)
N(31)−Fe−N(21)	96.75(8)
N(31)−Fe−N(11)	84.54(8)
N(21)−Fe−N(11)	84.64(8)
N(31)−Fe−N(11)	95.46(8)
N(21)−Fe−N(11)	95.36(8)
N(32)−C1−N(12)	111.75(19)
N(32)−C1−N(22)	111.75(19)
N(12)−C1−N(22)	111.38(19)

creases, because the bite size of these ligands is largely fixed, and increasing the tilting is an important way to accommodate larger metal ions.[10] In the fully high-spin structure[11] of {Fe[HC(3,5-Me$_2$pz)$_3$]$_2$}(BF$_4$)$_2$ this torsion angle averages 168°, with the range from 167.3 to 172.4°. In contrast, as is shown in Figure 2, in **1** two of the angles [178.92(16) and 179.74(16)°] suggest very little tilting, whereas the third ring shows substantial tilting with an angle of 164.55(15)°; the average value is 174.4°. The size of these angles is important: the angles are approximately 180° in these complexes when the iron(II) is low spin, and the Fe−N bond lengths are about 0.2 Å shorter.[10,13] Unfortunately, we have been unable to obtain the low-temperature crystal structure of **1** in order to follow how these angles change upon spin-state crossover, because the crystals shatter upon cooling to low temperature.

Magnetic Results

The temperature dependence of the molar magnetic susceptibility and the effective magnetic moment, μ_{eff}, of **1** is shown in Figure 3. This figure includes magnetic results for two full cycles of cooling and heating and reveals that the results for the second cooling and heating cycle are identical to those of the first cycle. Between 150 and 295 K the complex is paramagnetic and exhibits Curie law behavior with a Curie constant of 3.136 K/(emu/mol) and a small Weiss temperature of 1.85 K. These values correspond to an effective magnetic moment, μ_{eff}, of 5.01 μ_B between 150 and 295 K, a moment which is typical of high-spin iron(II) with a nominal octahedral $^5T_{2g}$ electronic ground state. Thus, above 150 K **1** is fully high spin.

As is shown in Figure 3, upon cooling below 150 K **1** exhibits a sharp decrease in its molar magnetic susceptibility beginning at about 110 K such that at 100 K and below the complex is essentially diamagnetic as would be expected of a low-spin iron(II) complex with a nominal octahedral $^1A_{1g}$ electronic ground state. Upon subsequent heating from 5 K, the complex remains low spin until, at 138 K, the magnetic susceptibility increases sharply such that at 148 K it is the same as that of the high-spin state. This behavior is typical of an iron(II) spin-state crossover, albeit with a rather large magnetic hysteresis of about 38 K.

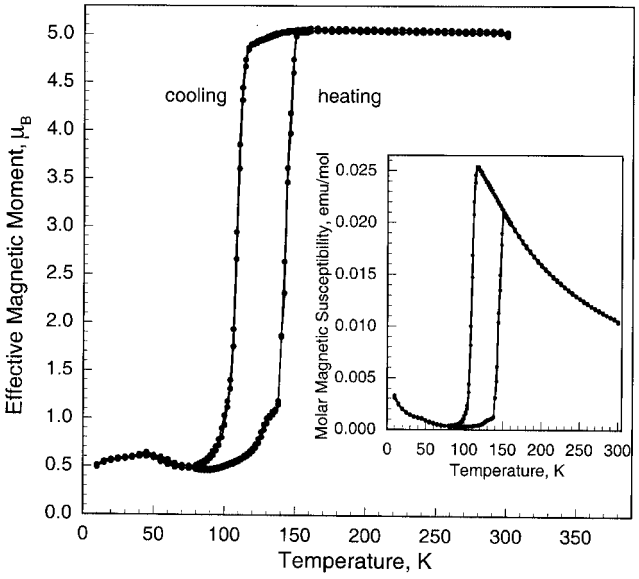

Figure 3. The temperature dependence of the effective magnetic moment of {Fe[HC(3,4,5-Me$_3$pz)$_3$]$_2$}(BF$_4$)$_2$ (**1**); inset: the temperature dependence of the molar magnetic susceptibility of **1**

Below about 60 K the molar magnetic susceptibility of **1** (see Figure 3) shows a small increase, which would be typical of an approximate 0.01 weight percent trace of either a high-spin iron(II) or a high-spin iron(III) impurity. Again, this behavior is typical of a diamagnetic complex whose low temperature magnetic properties are extremely sensitive to the presence of any paramagnetic impurities. Further, as is shown in Figure 3, below about 80 K the effective magnetic moment of **1** is essentially constant at 0.5 μ_B, a value which results partly from the trace impurity and predominately from a second-order Zeeman contribution to the molar magnetic susceptibility, i.e. the temperature-independent paramagnetic contribution to the moment of a diamagnetic complex that has a low-lying excited magnetic state; in this case the $^5T_{2g}$ state is the low-lying excited state at temperatures below the spin-state crossover.

Mössbauer Spectroscopic Results

The Mössbauer spectra of **1** obtained upon cooling from 296 K are shown in Figure 4, and the corresponding spectra obtained upon heating from 4.2 K are shown in Figure 5. In all cases the spectra have been fit with one or two symmetric quadrupole doublets, and selected hyperfine parameters are given in Table 3. The temperature dependence of the observed isomer shifts and quadrupole splittings is shown in Figure 6. The hyperfine parameters of the single quadrupole doublet observed at 160 K and above clearly indicate that **1** is high spin above this temperature.[2,7,11] Further, the hyperfine parameters of the single quadrupole

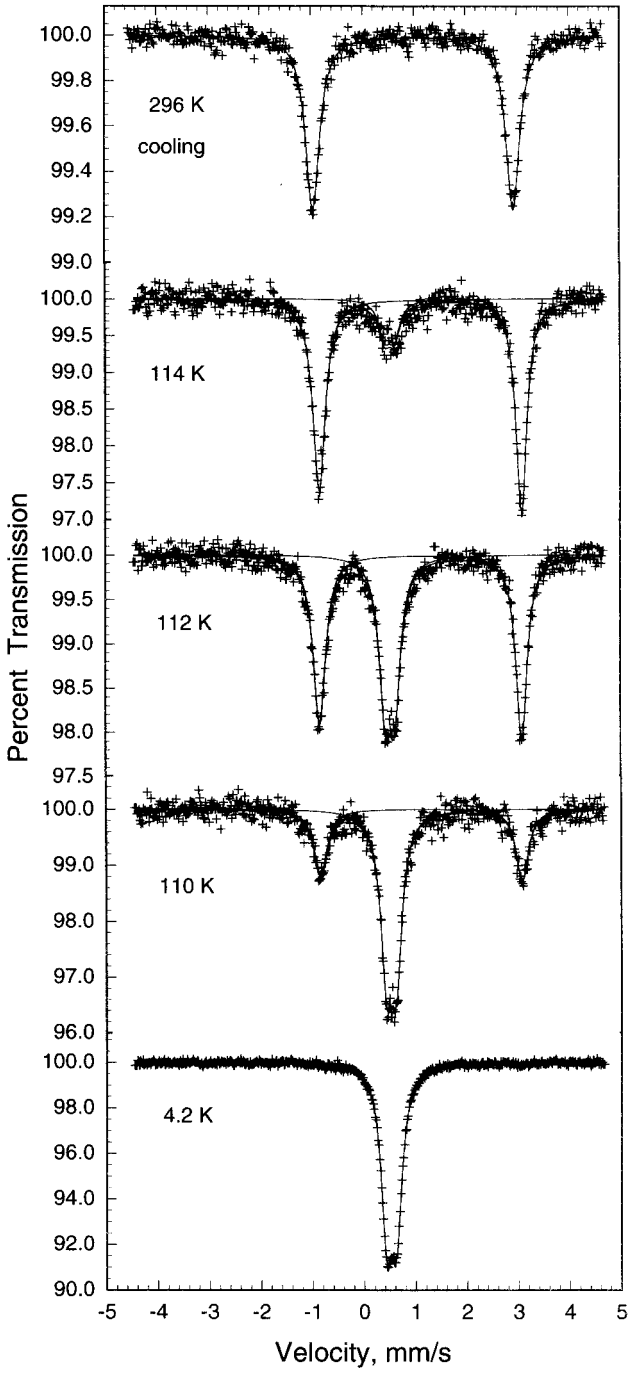

Figure 4. The Mössbauer spectra of {Fe[HC(3,4,5-$Me_3pz)_3]_2$}$(BF_4)_2$ (**1**) obtained at the indicated temperatures upon cooling from 296 K

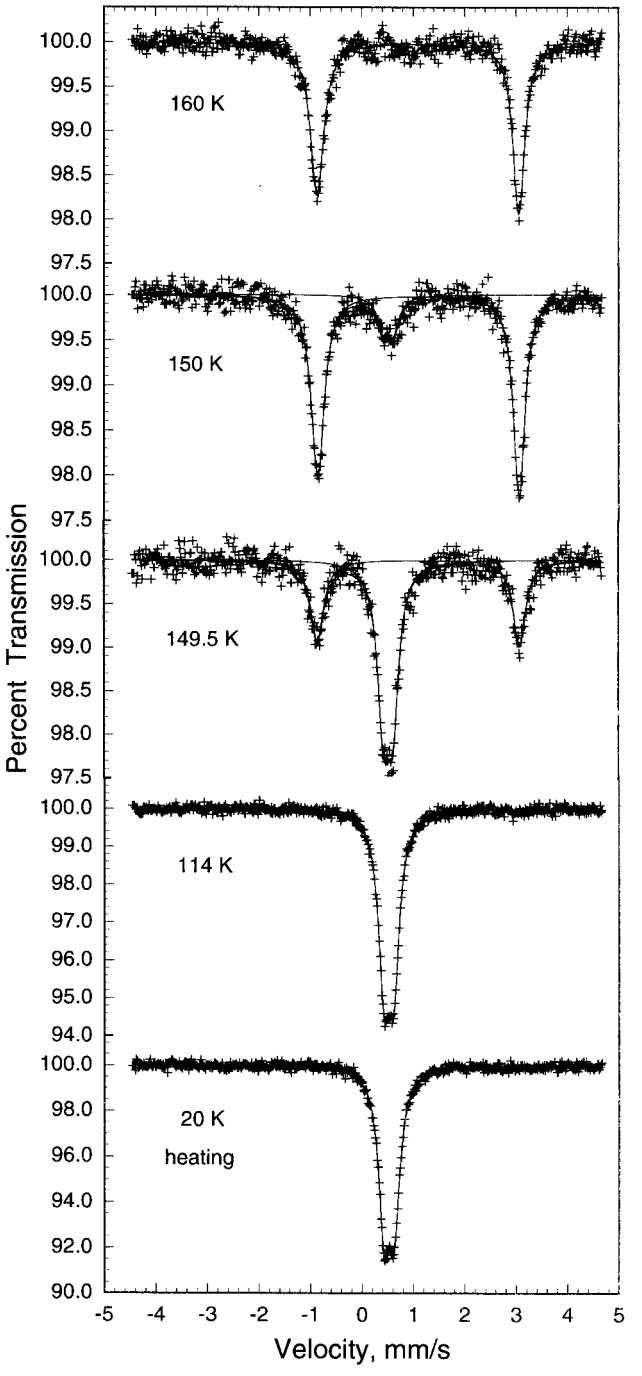

Figure 5. The Mössbauer spectra of {Fe[HC(3,4,5-$Me_3pz)_3]_2$}$(BF_4)_2$ (**1**) obtained at the indicated temperatures upon heating from 4.2 K

doublet observed between 4.2 and 100 K suggest that **1** is low spin at these temperatures. The linear temperature dependence of the high-spin isomer shift observed between 110 and 300 K is expected and, within the high-temperature limit, leads to an effective vibrating mass[19] of 64 g mol^{-1}. In the low-temperature limit, between 4 and 100 K, where the low-spin isomer shift is obtained, almost no temperature dependence of the isomer shift is observed, as expected.

The quadrupole splitting of approximately 3.9 mm s^{-1} observed for high-spin iron(II) is close to the maximum 4 mm s^{-1} expected[20] valence contribution to the quadrupole splitting, whereas the small quadrupole splitting of about 0.2 mm s^{-1} observed for the low-spin iron(II) results from the lattice contribution. The lattice contribution is usually opposite in sign to the valence contribution, and explains the reduction of the high-spin iron(II) quadrupole splitting from 4 to 3.9 mm s^{-1}. As expected, the low-spin quadrupole splitting resulting from the lattice contribution is virtually independent of temperature. Between 110 and 300 K the quadrupole splitting of the high-spin iron(II) does

Table 3. Selected Mössbauer spectroscopic hyperfine parameters

Complex	T (K)	δ[a] (mm s^{-1})	ΔE_Q (mm s^{-1})	Γ (mm s^{-1})	Area (%)	ε (%ε)/(mm s^{-1})	Assignment
{Fe[HC(3,4,5-Me$_3$pz)$_3$]$_2$}(BF$_4$)$_2$ (**1**)	296	1.002	3.89	0.28	100	0.662	HS
	114[b]	1.113	3.93	0.28	85.9	2.320	HS
		0.516	0.19	0.27	14.1	0.381	LS
	112[b]	1.113	3.93	0.28	57.6	1.695	HS
		0.516	0.19	0.27	42.4	1.245	LS
	110[b]]	1.112	3.92	0.30	34.2	1.132	HS
		0.523	0.19	0.27	65.8	2.178	LS
	100[b]	0.516	0.19	0.27	100	3.707	LS
	60[b]	0.522	0.20	0.27	100	4.506	LS
	20[b]	0.521	0.20	0.27	100	5.140	LS
	4.2	0.521	0.20	0.26	100	5.353	LS
	106[c]	0.516	0.19	0.26	100	3.419	LS
	114[c]	0.516	0.19	0.26	100	3.357	LS
	149.5[c]	1.100	3.93	0.30	38.7	0.870	HS
		0.513	0.18	0.27	61.3	1.381	LS
	150[c]	1.103	3.92	0.29	86.4	1.871	HS
	160[c]	1.093	3.92	0.28	100	1.662	HS
	220[c]	1.058	3.92	0.31	100	1.064	HS
{Fe[HC(3,5-Me$_2$pz)$_3$]$_2$}(BF$_4$)$_2$ (**2**)	295[d]	1.004	3.87	0.27	100	–	HS
	85[d]	1.131	3.88	0.26	50	–	HS
		0.529	0.20	0.26	50	–	LS
Fe[HB(3,5-Me$_2$pz)$_3$]$_2$ (**4**)	300[e]	1.03	3.65	0.33	100	–	HS
	78[e]	0.55	0.11	0.26	100	–	LS
Fe[HB(3,4,5-Me$_3$pz)$_3$]$_2$ (**3**)	293[e]	1.04	3.70	0.26	100	–	HS
	78[e]	1.13	3.72	0.26	100	–	HS
	4.2[e]	1.17	3.70	0.25	100	–	HS
	1.7[e]	1.20	3.71	0.29	100	–	HS

[a] The isomer shifts are given relative to room temperature α-iron foil. [b] Data obtained upon cooling from 296 K. [c] Data obtained upon heating from 4.2 K. [d] The average values obtained from Ref. 11. [e] Data obtained from Ref. 7.

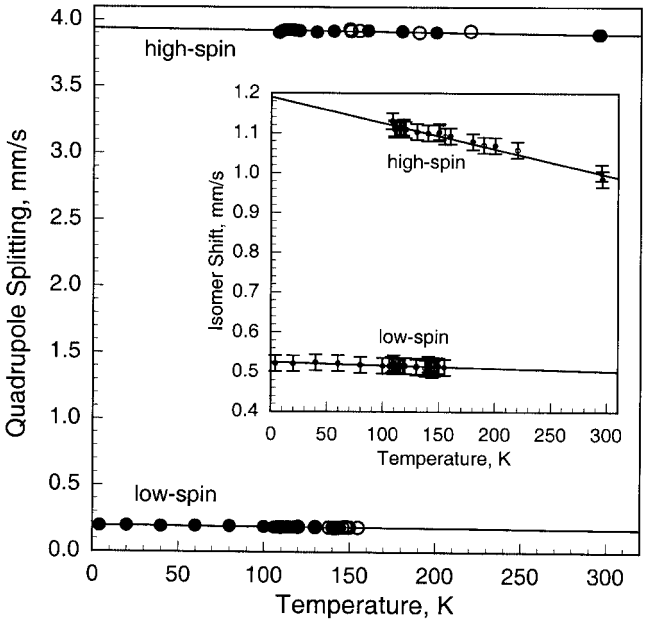

Figure 6. The temperature dependence of the Mössbauer spectroscopic quadrupole splitting of {Fe[HC(3,4,5-Me$_3$pz)$_3$]$_2$}(BF$_4$)$_2$ (**1**); inset: the temperature dependence of the isomer shift of **1**

not vary with temperature. Hence, the excited orbital states must lie at relatively high energy and are not thermally populated.

The population of the iron(II) high-spin state in **1** is shown in Figure 7 as a function of cooling from 295 to 4.2 K and subsequent heating from 4.2 to 240 K. Between 160 and 100 K the Mössbauer spectra of **1** exhibit two quadrupole doublets, which indicate the coexistence of the two electronic spin states at these temperatures. This spin-state coexistence is typical of a complex undergoing a spin-state crossover with a large thermal hysteresis; in this case a hysteresis of about 39 K is obtained, which agrees well with that (38 K) obtained from the magnetic studies (see above). It should be noted that there are both strong similarities and differences between the Mössbauer spectroscopic results for **1** and several related compounds. Although the hyperfine parameters of **1** are virtually identical to those of {Fe[HC(3,5-Me$_2$pz)$_3$]$_2$}(BF$_4$)$_2$ **2** (see Table 3), as would be expected on the basis of their very similar crystal structures at 150 and 220 K, respectively (see above), **1** undergoes a complete spin-state crossover with a distinct thermal hysteresis, whereas **2** shows no thermal hysteresis and is only 50 percent converted into the low-spin state, a conversion that is induced by the low-temperature phase transition.

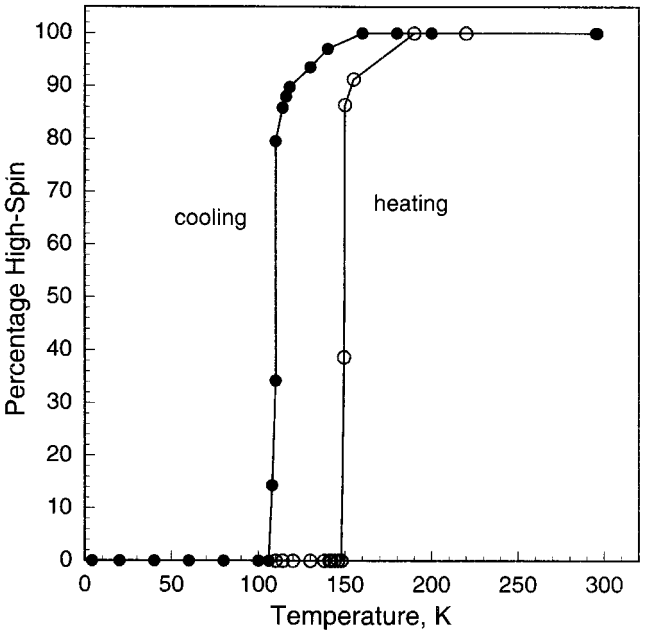

Figure 7. The percentage of high-spin iron(II) observed in the Mössbauer spectra of $\{Fe[HC(3,4,5\text{-}Me_3pz)_3]_2\}(BF_4)_2$ (**1**) as a function of temperature

Further, the structure of **1** is different from its analogous tris(pyrazolyl)borate complex, $Fe[HB(3,4,5\text{-}Me_3pz)_3]_2$ (**3**); the former shows a complete spin-state crossover upon cooling, whereas the latter does not exhibit any spin-state crossover and remains high-spin[7] even upon cooling to 1.7 K (see Table 3). The single-crystal X-ray structure of **3** has recently been determined,[21] and its structure has been found to be very similar to that of **1**, except that its average Fe−N bond length is 2.19 Å, i.e. it is 0.02 Å longer than that in **1**. This increase in the Fe−N bond length, which reduces the σ-electron density at the iron(II) in **3** relative to that in **1**, accounts for the significantly lower 295 K isomer shift observed in **1** than in $Fe[HB(3,4,5\text{-}Me_3pz)_3]_2$ (**3**) (see Table 3). Further, the distortion of the iron(II) coordination environment in **1** is found to be substantially larger[22,23] than that in **3**. The larger distortion accounts for the substantially larger quadrupole splitting observed in **1** relative to **3**. Finally, it should be noted that the spin-state crossover observed in **1** is similar to that observed in $Fe[HB(3,5\text{-}Me_2pz)_3]_2$ (**4**),[2,6,7] which shows a gradual spin-state crossover between 150 and 220 K, but again, the hyperfine parameters of **1** and **4** are somewhat different.

Because the temperature dependence of the Mössbauer spectra has been measured under identical conditions, i.e. a constant geometry and with a constant energy window, the changes in the spectroscopic absorption area as a function of temperature are directly related to the changes in the iron-57 recoil-free fraction. The logarithm of the total spectral absorption area observed in the Mössbauer spectra of **1** as a function of temperature is shown in Figure 8. The general decrease in ln(area) with increasing temperature is expected, but the jumps and hysteresis at approximately 110 K are unusual and are related to the spin-state crossover. The solid lines shown in Figure 8 correspond to a fit with the Debye model[19] between 4.2 and 100 K and between 150 and 296 K. These fits assume an effective vibrating mass of 57 g mol^{-1} and yield effective Mössbauer temperatures of 156 K for the low-spin state and 139 K for the high-spin state. The accuracy of these temperatures is estimated to be ± 10 K.

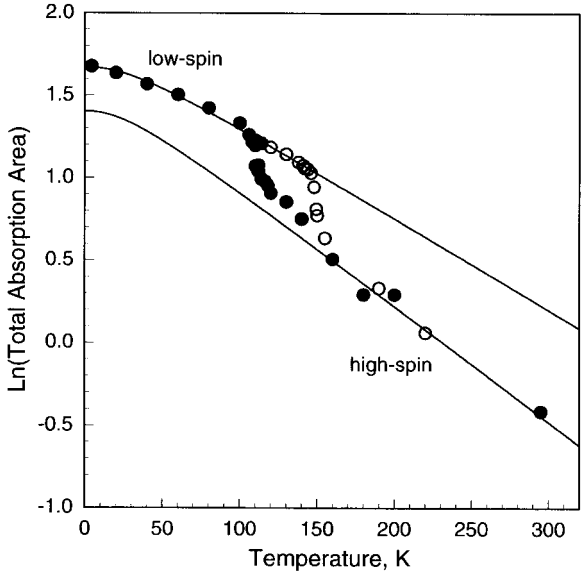

Figure 8. The logarithm of the total spectral absorption area observed in the Mössbauer spectra of $\{Fe[HC(3,4,5\text{-}Me_3pz)_3]_2\}(BF_4)_2$ (**1**) as a function of temperature; the straight lines correspond to the slope associated with the low-spin data obtained between 4.2 and 100 K and the high-spin data obtained between 160 and 296 K

The high-spin iron(II) ion in **1** has an average iron−nitrogen bond length of 2.162 Å, which is substantially larger than the typical value of 1.97 Å observed[9] for low-spin iron(II) complexes. The shorter average bond length leads to stronger bonding, more effective binding of the iron(II) ion into the lattice site, a higher recoil-free fraction, and a higher effective Mössbauer temperature for the low-spin iron(II) than for the high-spin iron(II) state.

Conclusions

The solid-state structure and color of $\{Fe[HC(3,4,5\text{-}Me_3pz)_3]_2\}(BF_4)_2$ clearly show that the complex contains high-spin iron(II) at ambient temperature. Both magnetic and Mössbauer studies show that the complex rapidly and completely changes to the low-spin state below 100 K. This behavior shows significant hysteresis upon heating where the change back to high spin does not begin until 138 K. This magnetic behavior is very different from the closely related complex $\{Fe[HC(3,5\text{-}Me_2pz)_3]_2\}(BF_4)_2$ that exhibits a spin-state crossover to the low-spin state of only one-half of the initially identical high-spin iron(II) ions and shows no hysteresis effects.[10−13] This very different behavior of $\{Fe[HC(3,4,5\text{-}Me_3pz)_3]_2\}(BF_4)_2$ is further evidence to sup-

port our earlier contention that the unusual spin-state crossover behavior of {Fe[HC(3,5-$Me_2pz)_3]_2$}$(BF_4)_2$ is completely controlled by the phase transition, one which prevents one-half of the initially identical high-spin iron(II) ions from changing to the low-spin form.

Experimental Section

Synthesis and Characterization: All operations were carried out under a nitrogen atmosphere using either standard Schlenk techniques or a dry box. All solvents were dried, degassed, and distilled prior to use. $Fe(BF_4)_2 \cdot 6H_2O$ was purchased from Aldrich. The synthesis of 3,4,5-trimethylpyrazole was performed according to a published method.[24]

Synthesis of tris(3,4,5-trimethylpyrazol-1-yl)methane: A 100 mL round-bottom flask was charged with 3,4,5-trimethylpyrazole (2.2 g, 20 mmol), tetra-*N*-butylammonium bromide (0.32 g, 1.0 mmol) and distilled H_2O (40 mL). Once the materials were dissolved, sodium carbonate (12.7 g, 120 mmol) was slowly added (*Caution: mildly exothermic reaction on addition*). Once the aqueous solution had cooled to near room temperature, chloroform (20 mL) was added to the flask. The flask was equipped with a reflux condenser and heated at a gentle reflux for 3 days, to give in a golden brown emulsion. The mixture was allowed to cool to room temperature, filtered through a Büchner funnel to remove the excess base, and the organic layer separated from the aqueous layer. The organic layer was washed with distilled water (2 × 10 mL) and dried over sodium sulfate. The drying agent was removed by filtration, and the solvent removed by rotary evaporation. The resulting oily, brown solid was flushed through a plug of silica with chloroform (2 × 100 mL) to afford a pale yellow solid (1.4 g, 62%). M.p. 156−157 °C (literature[18]: 156−157 °C). ^{1}H NMR ($CDCl_3$): δ = 186, 1.92 (3,5-CH_3, s, s; 9 H, 9 H,), 2.12 (4-CH_3, s, 9 H), 8.03 (C*H*, s, 1 H) ppm.

Synthesis of {Fe[HC(3,4,5-$Me_3pz)_3]_2$}$(BF_4)_2$: A 50 mL round-bottom Schlenk flask was charged with $Fe(BF_4)_2 \cdot 6H_2O$ (0.200 g, 0.60 mmol) and distilled THF (3 mL) was added with the use of a syringe. A second 50 mL round-bottom Schlenk flask was charged with tris(3,4,5-trimethylpyrazol-1-yl)methane (0.500 g, 1.5 mmol) and distilled THF (6 mL) was added by a syringe. Once the starting materials were dissolved, the ligand/THF solution was added to the metal/THF solution by cannula transfer. The resulting mixture was left to stir overnight, yielding a white powder precipitate. The solvent was removed by cannula filtration, and the solid was washed with distilled hexane and dried under vacuum (0.47 g, 85% yield). M.p.: decomposes above 318 °C. ^{1}H NMR ([D_6]acetone): δ = 41.2, 20.9, 7.4 (18, 18, 18, v. br., br., br., Me_3), −42.8 (2, v. br., *H*−C). TOF MS ES+: *m*/*z* calcd. for {Fe[HC(3,4,5-$Me_3pz)_3]_2$}$(BF_4)^+$: 823.4129; found: 823.4132. Elemental Analysis: calcd. C 49.79, H 6.19, N 18.34; found C 49.21, H 6.21, N 18.43. Crystals for X-ray crystallographic and magnetic analysis, and Mössbauer spectroscopy were grown by layering a saturated acetone solution with hexane.

X-ray Structure Determination of {Fe[HC(3,4,5-$Me_3pz)_3]_2$}$(BF_4)_2 \cdot 0.35H_2O$: A colorless block crystal was mounted onto the end of a thin glass fiber using inert oil. X-ray intensity data covering the full sphere of reciprocal space were obtained at 150(1) K on a Bruker SMART APEX CCD-based diffractometer with Mo-K_α radiation, λ = 0.71073 Å.[25] The raw data frames were integrated with SAINT+,[25] which also corrected for Lorentz polarization effects. The final unit cell parameters are based on the least-squares refinement of 6654 reflections from the data set with $I > 5(\sigma)I$. Analysis of the data showed negligible crystal decay during data collection. An empirical absorption correction, based on the multiple measurement of equivalent reflections, was applied with the program SADABS.[25]

{Fe[HC(3,4,5-$Me_3pz)_3]_2$}$(BF_4)_2 \cdot 0.35H_2O$ crystallizes in the triclinic system and the structure was solved in the $P-1$ space group through a combination of direct methods and difference Fourier syntheses and refined by full-matrix least-squares against F^2 by using the SHELXTL software package.[26] The {Fe[HC(3,4,5-$Me_3pz)_3]_2$}$^{2+}$ cation resides on a center of symmetry and the BF_4^- counterion is rotationally disordered; a model incorporating four distinct orientations of the BF_4^- anion was used in the refinement. A total of 68 restraints were employed to maintain a chemically reasonable geometry for the disordered components. Initially, the site occupation factors for the four components were allowed to refine freely, but were subsequently fixed at the refined values and then adjusted slightly to sum to unity (0.38, 0.39, 0.14, 0.09). Atoms of the two minor components were refined with only isotropic displacement parameters. A significant, isolated electron-density peak present near the end of the refinement was assumed to be a partially occupied water molecule, which refined to a 35% occupancy; its hydrogen atoms were not located or calculated. All non-hydrogen atoms, except for the BF_4^- atoms mentioned above, were refined with anisotropic displacement parameters. Hydrogen atoms were placed in geometrically idealized positions and refined as standard riding atoms.

It was not possible to obtain the single-crystal X-ray structure of {Fe[HC(3,4,5-$Me_3pz)_3]_2$}$(BF_4)_2$ (**1**) in the low-spin state, because the crystals always shattered upon cooling through the spin-state crossover. Further, changes in the magnetic behavior of the compound upon grinding prevented the measurement of the powder diffraction pattern of the complex at low temperature in the low-spin state.

Magnetic Measurements: Magnetic susceptibilities were measured on crystalline samples at 0.5 T by using a Quantum Design MPMS XL SQUID magnetometer. Clear gelatine capsules were used as sample containers for measurements between 5 and 350 K. The very small diamagnetic contribution of the gelatine capsule had a negligible contribution to the overall magnetization which was dominated by the sample. The molar magnetic susceptibilities were corrected for the diamagnetic susceptibility of {Fe[HC(3,4,5-$Me_3pz)_3]_2$}$(BF_4)_2$ by using the value of −0.0004632 emu/mol that was obtained from Pascal's constants.

Mössbauer Spectroscopic Measurements: The Mössbauer spectroscopic absorber contained 50 mg/cm^2 of powder mixed with boron nitride, and the spectra were measured between 4.2 and 295 K on a constant-acceleration spectrometer which utilized a room-temperature rhodium-matrix cobalt-57 source and was calibrated at room temperature with α-iron foil. The estimated absolute errors are ± 0.005 mm/s for the isomer shifts, ± 0.01 mm/s for the quadrupole splittings and line widths, and ± 0.2 percent for the relative spectral absorption areas.

Acknowledgments

G. J. L. thanks the Francqui Foundation of Belgium for his appointment as a "Chaire Francqui Interuniversitaire au titre étranger" during the 2002−2003 academic year. The authors also acknowledge with thanks the financial support of the US National Science Foundation through grant CHE-0110493 for D. L. R. and

DMR-9521739 for G. J. L. and the Fonds National de la Recherche Scientifique, Belgium, through grant 9.456595, and the Fonds de la Recherche Fondamentale Collective, Belgium, through grants 2.4531.00F and 2.4522.01. L. R. and F. G. thank the Ministère de la Région Wallonne for grant RW/115012.

[1] S. Trofimenko, *Scorpionates: The Coordination Chemistry of Polypyrazolylborate Ligands*, Imperial College Press, London, **1999**.
[2] G. J. Long, F. Grandjean, D. L. Reger, in *Spin Crossover in Transition Metal Compounds* (Eds.: P. Gütlich, H. A. Goodwin), Springer, Berlin, **2004**, in press.
[3] P. Gütlich, A. Hauser, H. Spiering, *Angew. Chem. Int. Ed. Engl.* **1994**, *33*, 2024−2054 and references cited therein.
[4] F. A. Cotton, J. Wilkinson, C. A. Murillo, M. Bochmann, *Advanced Inorganic Chemistry* (6th ed.), John Wiley & Sons, New York, **1999**, pp. 785−786.
[5] J. P. Jesson, S. Trofimenko, D. R. Eaton, *J. Am. Chem. Soc.* **1967**, *89*, 3158−3164.
[6] J. P. Jesson, J. F. Weiher, S. Trofimenko, *J. Chem. Phys.* **1968**, *48*, 2058−2066.
[7] G. J. Long, B. B. Hutchinson, *Inorg. Chem.* **1987**, *26*, 608−613.
[8] F. Grandjean, G. J. Long, B. B. Hutchinson, I. Ohlhausen, P. Neill, J. D. Holcomb, *Inorg. Chem.* **1989**, *28*, 4406−4414.
[9] C. Hannay, M.-J. Hubin-Franskin, F. Grandjean, V. Briois, J.-P. Itié, A. Polian, S. Trofimenko, G. J. Long, *Inorg. Chem.* **1997**, *36*, 5580−5588.
[10] D. L. Reger, C. A. Little, A. L. Rheingold, M. Lam, T. Concolino, A. Mohan, G. J. Long, *Inorg. Chem.* **2000**, *39*, 4674−4675.
[11] D. L. Reger, C. A. Little, A. L. Rheingold, M. Lam, L. M. Liable-Sands, B. Rhagitan, T. Concolino, A. Mohan, G. J. Long, V. Briois, F. Grandjean, *Inorg. Chem.* **2001**, *40*, 1508−1520.
[12] D. L. Reger, C. A. Little, V. G. Young Jr., M. Pink, *Inorg. Chem.* **2001**, *40*, 2870−2874.
[13] D. L. Reger, C. A. Little, M. D. Smith, G. J. Long, *Inorg. Chem.* **2002**, *41*, 4453−4460.
[14] D. L. Reger, C. A. Little, M. D. Smith, A. L. Rheingold, K.-C. Lam, T. L. Concolino, G. J. Long, R. P. Hermann, F. Grandjean, *Eur. J. Inorg. Chem.* **2002**, 1190−1197.
[15] C. Piquer, F. Grandjean, O. Mathon, S. Pascarelli, D. L. Reger, C. Little, G. J. Long, *Inorg. Chem.* **2003**, *42*, 982−985.
[16] V. Briois, P. Sainctavit, G. J. Long, F. Grandjean, *Inorg. Chem.* **2001**, *40*, 912−918.
[17] D. L. Reger, C. A. Little, A. L. Rheingold, R. Sommer, G. J. Long, *Inorg. Chim. Acta* **2001**, *316*, 65−70.
[18] C. Pettinari, M. Pellei, A. Cingolani, D. Martini, A. Drozdov, S. Troyanov, W. Panzeri, A. Mele, *Inorg. Chem.* **1999**, *38*, 5777−5787.
[19] R. H. Herber, in *Chemical Mössbauer Spectroscopy* (Ed.: R. H. Herber), Plenum; New York, **1984**, pp. 199−216.
[20] D. C. Price, F. Varret, *Studies Physical Theoretical Chem.: Adv. Mössbauer Spectroscopy* **1983**, *25*, 316−397.
[21] D. L. Reger, J. R. Gardinier, M. D. Smith, unpublished results.
[22] The Fe−N bond and N−Fe−N angular distortion parameters[23] are 0.491 and 6.51 percent for **1** and 0.107 and 4.25 percent for **2**.
[23] B. Renner, G. Lehmann, *Z. Krist.* **1986**, *175*, 43−59.
[24] A. Wlodarczyk, R. M. Richardson, M. D. Ward, J. A. McCleverty, *Polyhedron* **1996**, *15*, 27−35.
[25] SMART Version 5.625, SAINT+ Version 6.02a and SADABS. Bruker Analytical X-ray Systems Inc., Madison, Wisconsin, USA, **1998**.
[26] Sheldrick, G. M., SHELXTL Version 5.1, Bruker Analytical X-ray Systems Inc., Madison, Wisconsin, USA, **1997**.

Received December 30, 2003
Early View Article
Published Online June 1, 2004

